VDMA
Fluid Power Association

23rd ISC

International Sealing Conference

Stuttgart, Germany
Sept.30 - Oct.1, 2026

Sealing the future –
Facing the challenges of tomorrow

UNI STUTTGART

© 2026 VDMA Fluidtechnik
All rights reserved. No part of this publication may be reproduced, stored in retrieval systems or transmitted in any form by any means without the prior permission of the publisher.

Fachverband Fluidtechnik im VDMA e. V. Lyoner Str. 18
50628 Frankfurt am Main
Germany

Phone +49 69 6603-1513
E-Mail maximilian.baxmann@vdma.eu

Internet www.vdma.eu/fluid

Experimental Study on Lubrication Film Characteristics of Grease-Lubricated Radial Seals under Oscillating Motion Using Fluorescence Microscopy

Takao Horiuchi, Yohei Sakai, Syunsuke Sato, Ayako Aoyagi

The grease-sealing mechanism of radial seals during the oscillating operation of industrial robots and similar equipment was observed in situ using the fluorescence method. Individual evaluation of the film thickness fluctuations of the base oil and the thickener on the sliding surface revealed that they exhibited different flow behaviors. Due to insufficient oil bleeding and thickener stacking, flow was unstable under short-cycle oscillation. By contrast, long-cycle oscillation stabilized the film thickness fluctuation; the fluid fluctuated at approximately the same frequency as the shaft motion, and successful sealing was achieved through the optimal balance between the shear-induced fluidization of the grease and the sufficient sliding distance for pumping.

1 Introduction

The joints of industrial robots are driven by servo motors and reduction gears. Grease lubrication of reduction gears is important for precise robot movement, and radial seals prevent grease leakage. The sealing mechanism of these products under oil lubrication has been investigated by many researchers and is well understood [1]. However, most of the sealing principle is unclear in cases where grease is used during oscillating operation. Researchers have suggested that thickener particles interpose within clearances on these seals, affecting their sealing abilities [2]. Therefore, the behaviors of the base oil and the thickener should be observed individually to understand the underlying grease-sealing mechanisms. Sato observed the lubrication film of radial seals under oil lubrication using laser-induced fluorescence [3]. However, their work was limited to oil-lubricated systems. Infrared spectroscopy and fluorescence methods are effective techniques for separately observing the behaviors of base oils and thickeners in situ [4], [5]. Thus, in the present study, the behaviors of the base oil and the thickener on the seal sliding surface were observed via the fluorescence method. The film thickness distribution on the sliding surface differs between the base oil and the thickener when grease is sealed [6]. However, the effect of this flow difference on sealing abilities during oscillating operation is unclear. This work thus measures the film thicknesses of the base oil and the thickener on the seal sliding surface using the fluorescence method and investigates their correlations with actual shaft motion.

2 Materials and Methods

Fluid behavior during oscillating operation was examined by measuring the film thicknesses of the base oil and the thickener, along with the film thickness gradient, using the fluorescence method while tracking the actual shaft motion using a marker attached to the shaft.

2.1 Sample

FKM-based radial seals were subjected to sealing tests. A schematic diagram of the seal geometry is shown in Figure 1. The measured surface roughness of the seal lip was Ra = 1.02 µm (and Rz = 6.45 µm). Lithium soap grease with a thickener concentration of 6.6%, a National Lubricating Grease Institute grade of 2, and a base oil viscosity of 30 cSt at 40°C was used. The fluorescent agents perylene and rhodamine B were used to separately observe the base oil and the thickener, respectively.

2.2 Operation

Tests were conducted under the four oscillating operating patterns shown in Table 2 to investigate the effects of oscillating frequency and speed on base oil and thickener behaviors. The acceleration/deceleration time, 0.1 s, was included in the sliding time. A stop time of 0.1 s was set between the clockwise (CW) and counterclockwise (CCW) rotations. Under each condition, measurements were performed after approximately 12 h of running-in to ensure stable leakage to the air side.

2.3 Sealing Performance Assessment

Sealing performance was quantitatively evaluated by measuring the leakage amount and pumping rate per cycle (Table 2). Each test was conducted for approximately 72 h using a hollow glass shaft. Unlike during fluorescence observation, simple reflection images were captured using a white light source. The leakage width was measured from the meniscus of the grease that leaked to the air side, and the leakage volume was subsequently calculated based on the deformed seal profile. Furthermore, the pumping rate was determined by installing the radial seal in the reverse orientation and similarly evaluating the volume of the discharged grease.

2.4 Fluorescence Observation

Figure 2 shows a schematic of the testing machine used for fluorescence observation. Two radial seals were installed in a housing, and fluorescent grease for tests was injected between them from one of two holes drilled into the housing. After grease injection, one hole was closed, and the setup was left to rest for at least 24 h before the tests to prevent internal pressure from developing. The sliding surface was observed from the inside of the hollow glass shaft, which had an average roughness of Ra = 0.006 µm (Rz = 0.007 µm). The operational principle of fluorescence measurement relied on the distinction between the base oil and thickener phases under selective wavelength excitation, following established methodologies [5], [7]. The light source was a mercury–xenon lamp with a dichroic mirror and an excitation filter. The excitation filter selected a specific wavelength band to excite the fluorescent agents dissolved in the grease, and the dichroic mirror reflected this excitation light toward the interface. The fluorescence emitted from the sliding surface passed back through the dichroic mirror and an emission filter, which effectively cut off the scattered excitation light. Table 1 summarizes the optical properties of the fluorescent agents, including their excitation and emission peaks, and the specifications of the excitation filters, dichroic mirrors, and emission filters. Crosstalk between the base oil and thickener fluorescence was effectively eliminated by strictly separating these wavelength bands. Only the fluorescence image was thus captured using a CMOS camera with an exposure time of 30 ms and a frame rate of up to 33 fps.

2.5 Calibration

Film thickness was quantitatively evaluated from the fluorescence images by performing prior calibration and image correction as follows. First, a fluorescence image between the two grease-filled seals was obtained to create an illuminance distribution map and eliminate the influence of the spatial intensity distribution of the light source. Each obtained fluorescence image was corrected by dividing it by the normalized shading map to achieve equivalence with uniform light-source irradiation [7]. A calibration curve was created as follows: an FKM sheet prepared from the material used for the seals was placed at an inclination angle of 1°, and lubricant was applied on top and pressed with a glass plate to obtain a fluorescence image. In situ verification was also performed to confirm calibration accuracy. Because the oil side of the seal was completely filled with the lubricant, the calibration curve for the actual machine conditions was obtained under the assumption that the oil film thickness varied according to the sealing profile with the shaft inserted. The deviations of the coefficients were checked before and after the tests. The error range was approximately 10–100 nm.

The thickener was calibrated using a method similar to the above. However, given the technical difficulty of strictly quantifying the thickener component, the calibration curve was calculated based on the assumption that "within the calibration acquisition range, the thickener is uniformly dispersed according to the initial concentration of the grease." Therefore, the presented thickener film thicknesses are normalized fluorescence intensities, enabling a relative cross-condition comparison based on this assumption.

Figure 3 shows a cross-sectional view of the film thickness distribution calculated from the obtained fluorescence images. The gradient of the film thickness differed between the sliding surface and the air or oil side. Hence, the boundaries between the sliding surface and the oil and air sides were identified by detecting the maximum gradient around these regions. The average film thickness on the sliding surface was calculated from the average values in the ±12 μm area from the center of each boundary (green area in Figure 3). Additionally, the film thickness gradient of the base oil during operation was obtained from the film thickness profiles of the base oil and the thickener between both boundaries.

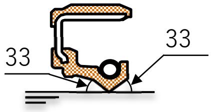

Figure 1: Schematic Diagram of Seal Geometry

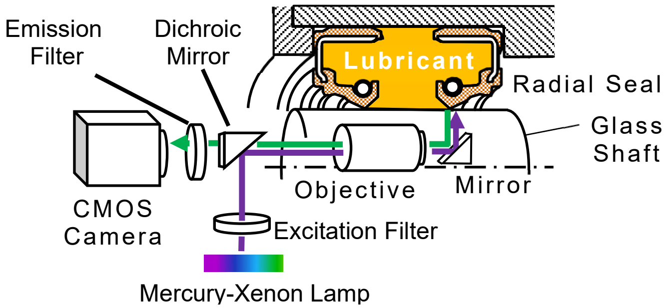

Figure 2: Schematic of Test Rig

Table 1: Optical Properties of Fluorescent Agents

Fluorescent agent	Perylene (for base oil)	Rhodamine B (for thickener)
Excitation peak	444 nm	544 nm
Emission	465 nm	562 nm
Excitation filter	435/40 nm	543/22 nm
Dichroic mirror	458 nm	562 nm
Emission filter	482.5/36 nm	575/22 nm

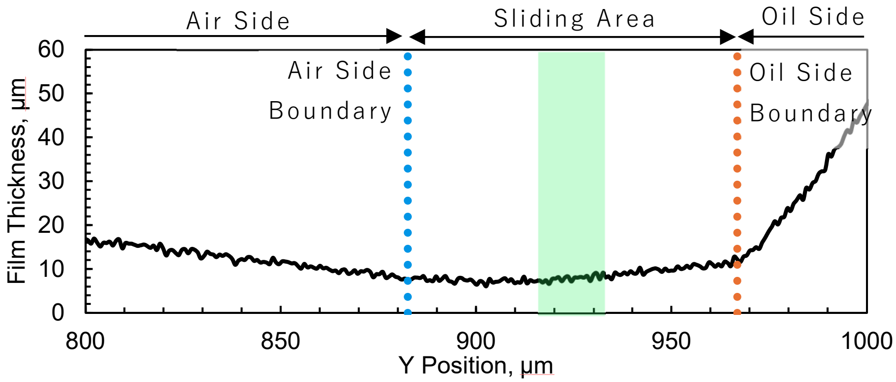

Figure 3: Cross-Sectional Profile of Film Thickness Distribution

Table 2: Operating Conditions and Seal Test Results

	A	B	C	D
Axial eccentricity	TIR 0.03 mm			
Sliding speed	Max 0.13 m/s (30 rpm)			
Maximum acceleration	0.46 m/s^2	0.72 m/s^2	0.66 m/s^2	1.80 m/s^2
Sliding time	0.3 s	0.5 s	0.7 s	1.2 s
Operation program	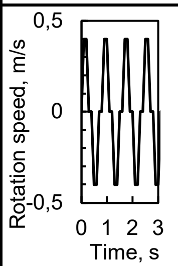	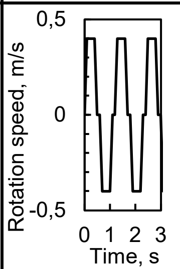	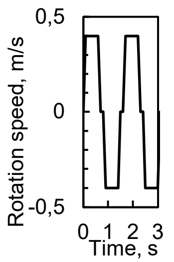	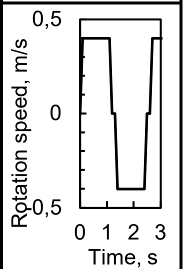
Leakage amount/cycle	0.0011 µm^3	0.00012 µm^3	0.00063 µm^3	0 µm^3
Pumping rate/cycle	4.19 µm^3	27.11 µm^3	31.36 µm^3	45.26 µm^3

Note: TIR: total indicator reading.

3 Test Results

The film thickness on the sliding surface obtained via the fluorescence method and the actual shaft motion were measured independently. Their correlation was evaluated by synchronizing their time axes by aligning the operation start point. The fluorescence images were continuously acquired for approximately 40 s from the start of the operation. The dynamic fluid behavior was quantitatively evaluated through two types of frequency analyses. Before these analyses, zero-mean processing was applied to the obtained time-series data to remove the DC component. First, overall fast Fourier transform analysis was conducted using the entire 40 s data to determine the dominant fluctuation frequency for each parameter, which was defined as the frequency with the maximum amplitude. Second, the temporal transition of these frequencies was visualized by generating spectrograms using short-time Fourier transform. These spectrograms were computed using a Hamming window of 256 points, sliding in 0.3 s increments. This window size provided a frequency resolution of approximately 0.129 Hz.

3.1 Sealing Performance

Table 2 summarizes sealing performance at 30 rpm. While the pumping rate increased proportionally with sliding time (A < B < C < D), the leakage amount exhibited a nonlinear trend (A > C > B > D). Therefore, a higher pumping capacity did not straightforwardly reduce leakage, highlighting a complex sealing mechanism during oscillating operation.

3.2 Observation Images

Figure 4 shows a 2D mapping image of the film thickness distribution under condition A. The base oil and the thickener on the sliding surface exhibited different film thickness distributions [6]. The base oil showed a gradual film thickness gradient from the oil side to the sliding surface and further leaked to the air side. The 2D mapping image of the thickener indicated that the thickener penetrated the sliding surface from the oil side. Furthermore, the thickener leaked to the air side, although its leakage amount was small. These results confirmed that the thickener and the base oil did not exhibit the same flow behavior.

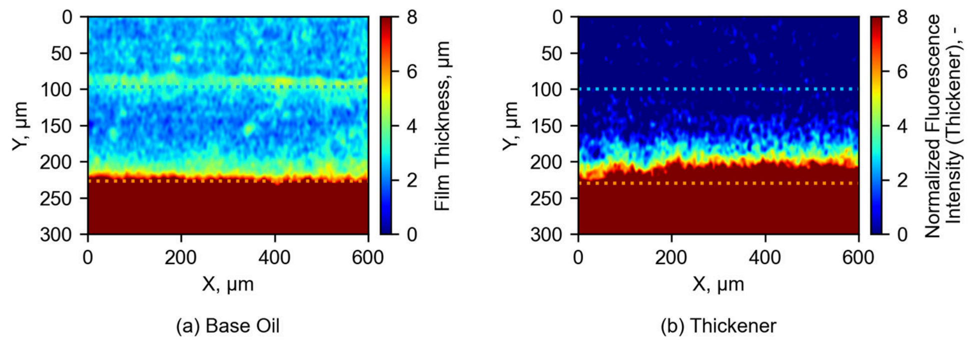

Figure 4: Film Thickness Distribution at 6 s after Operation Start (Operating Condition A)

3.3 *Effect of Sliding Time*

Figure 5 shows the measurement results for the initial 6 s of operation at a constant maximum speed of 30 rpm with varying sliding times. The blue-shaded graphs indicate parameters fluctuating at approximately the same frequency as the shaft motion, whereas those shaded red indicate fluctuations at double the shaft frequency.

Regarding the base oil’s film thickness, fluctuations occurred at approximately the same frequency as the shaft motion across all conditions. Figure 6 shows the spectrogram corresponding to each condition. Under conditions A and D, the fluctuation amplitudes were initially small but exhibited distinct transient behaviors over time. Under condition A, the amplitude gradually increased after approximately 5 s of operation and began fluctuating at approximately the same frequency as the shaft motion (0.37 Hz). Under condition D, although the amplitude remained small, the fluid began fluctuating at approximately the shaft frequency (0.37 Hz) from around 3 s. After approximately 12 s, the dominant fluctuation frequency under condition D doubled from 0.37 Hz to 0.74 Hz. Furthermore, the fluctuation pattern became unstable and irregular after around 26 s. Under conditions B and C, the base oil film thickness fluctuated at approximately the same frequency as the shaft motion from the beginning of the operation.

As for thickener behavior, the normalized fluorescence intensity on the sliding surface fluctuated at approximately the same frequency as the shaft motion under conditions A, B, and C. Although the thickener fluctuation frequency under condition D remained completely stable throughout the 40 s operation, not showing any frequency doubling or instability, the film thickness gradient of the base oil exhibited the same timing of frequency doubling as the base oil film thickness.

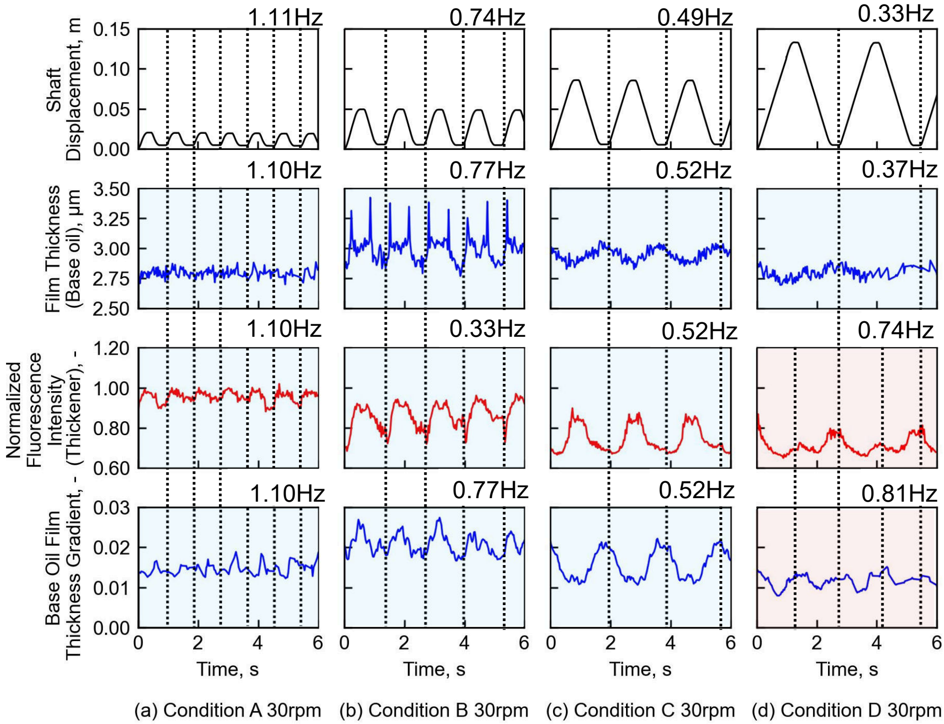

Figure 5: Measurement Results at Varying Sliding Times

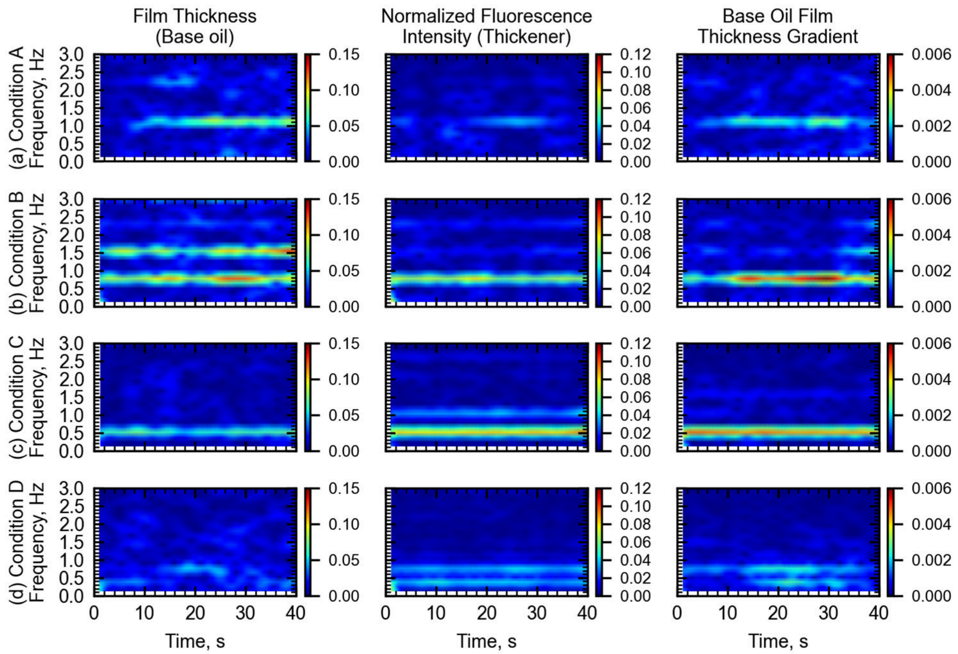

Figure 6: Spectrograms Showing Temporal Transitions of Fluctuation Frequencies

4 Discussion

The above measurement results show that the grease rheological properties, which govern lubrication film formation, behave differently, depending on the sliding time under the grease lubrication of radial seals.

4.1 Delayed Fluid Fluctuation

The spectrograms for conditions A and D (Figure 6) reveal distinctly delayed fluid fluctuations. Under condition A, the base oil film thickness did not exhibit clear frequency characteristics for approximately 5 s. The thickener's intermittent instability suggested that the initial bleeding of the highly fluid oil was insufficient. The bled oil flowed at the shaft frequency, but the flowability loss and stagnation (stacking) of the thickener caused instability. Under condition D, despite the slight initial oil bleeding, some time was needed to break down the thickener network for proper flow.

4.2 Thickener Accumulation in Short-Cycle Oscillation

The 2D mapping image in Figure 4 shows that the thickener penetrated the sliding surface from the oil side. Under short-cycle conditions, such as condition A, the thickener was continuously drawn into the contact area but encountered low applied shear. Consequently, the thickener could not circulate back or flow through, thereby gradually stagnating and stacking on the sliding surface. This stacking mechanism is strongly supported by the continuous increase in the thickener amount in Figure 5 and its unstable fluctuation frequency in Figure 6. Breaking down this stacked network to restore flow took time, causing unstable fluctuations.

Under condition B, sufficient shear allowed the grease to flow stably at the shaft frequency from the start of the operation despite local accumulation. Furthermore, the base oil film thickness under condition B exhibited a stably doubled frequency with the largest fluctuation amplitude. Thus, a large amount of oil dynamically moved in and out of the sliding surface during CW and CCW rotations, but the moderate network breakdown maintained enough viscosity to prevent the oil from leaking to the air side.

As the sliding distance increased, the amplitude of the thickener’s doubled frequency gradually became almost equal to that of the shaft frequency. This provides direct evidence that the thickener network breakdown progressed highly and more uniformly in both stroke directions with longer strokes. Condition C exhibited more leakage than condition B because the highly fluidized grease easily escaped the sealing gap, as the outward leakage flow exceeded the available pumping capacity. Finally, Condition D’s overwhelming pumping rate pulled back the highly fluidized grease, preventing leakage.

Thus, successful sealing requires a delicate balance: once shear highly fluidizes the thickener network, the sliding stroke must generate sufficient pumping capacity to overcome the grease’s tendency to leak due to viscosity loss.

4.3 Influence of Continuous Pumping

The base oil exhibited a notable transient behavior under condition D (Figure 6): frequency doubling at 12 s and instability after 26 s. Given the stable fluctuation frequency of the thickener, this instability stemmed not from the grease property changes but from the high pumping rate, which continuously drew the sliding surface oil toward the oil side. A comparison of the base oil film thickness gradients supports this strong pumping effect. Under condition B, although the base oil film thickness fluctuated significantly at the doubled frequency, the gradient’s weak fluctuation at the doubled frequency implied that the oil merely moved back and forth, without strong directional pumping. By contrast, the gradient under condition D fluctuated at the doubled frequency from the beginning, and after 12 s, the shaft frequency appeared alongside it. Thus, as the strong continuous pumping progressed, the rapid cyclic fluctuations of the base oil stabilized into a steady periodic behavior synchronized with the shaft motion, heavily influenced by the inward pumping flow.

Furthermore, as demonstrated by the 40 s time-series profile of condition D in Figure 7, the average base oil film thickness did not decrease over time, even after the fluctuation pattern became unstable at 26 s. This sustained film thickness was achieved because the test was conducted after promoting leakage during the 12 h running-in process, which allowed for a continuous secondary oil supply from the air side under strong pumping. Therefore, the fluctuation instability after 26 s was attributed to active fluid exchange and dynamic recirculation between the oil and air sides driven by the continuous pumping. Additionally, the small overall fluctuation amplitude of the base oil film thickness under condition D indicated that the oil was continuously drawn inward, aided by the inertial forces maintaining the flow during momentary stops. Therefore, even with microscopic instabilities in the base oil's flow due to dynamic recirculation, sealing was maintained as long as the macroscopic thickener network flowed stably, without local accumulation.

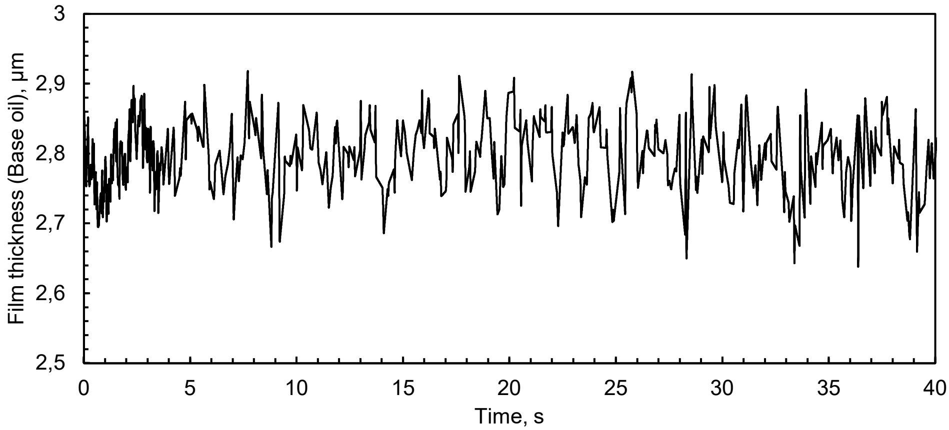

Figure 7: Time-Series Profile of Base Oil Film Thickness under Condition D

5 Conclusion and Outlook

In this study, the grease-sealing mechanism of radial seals during oscillating operation was investigated via in situ fluorescence observation and time-frequency analysis. Sealing performance heavily relies on achieving a fluid-like state, which requires sufficient shear to break down the thickener network and reduce its viscosity. Without this state, grease stagnates and stacks, causing leakage.

Successful sealing requires an optimal balance between the shear-induced fluidization of the thickener network and a sliding stroke that can generate pumping capacity that surpasses the grease's leakage tendency. Furthermore, under long-stroke conditions, a strong pumping effect continuously draws oil inward, driven by inertial forces. These findings suggest that optimizing operational stroke programs and grease rheological properties improves sealing reliability.

Future studies will investigate different grease formulations and rubber materials to elucidate the detailed relationship between seal dynamics and transient grease accumulation.

6 References

[1] Jagger,E.T.: Rotary shaft seals: the sealing mechanism of synthetic rubber seals running at atmospheric pressure, In: Proceedings of the Institution of Mechanical Engineers, Vol. 171/1, pp. 597-616, 1957

[2] Sommer, M., Haas, W.: A new approach on grease tribology in sealing technology: Influence of the thickener particles, In: Tribology International, Vol. 103, pp. 574-583, 2016

[3] Sato,Y.: *Study of Lubrication Mechanism on Oil Seals*, Kyushu University, 2001

[4] Hoshi, Y., Takiwatari, K., Nanao, H., Mori, S.: In situ observation of transient responses in grease lubrication by micro infrared spectroscopy, In: Journal of Japanese Society of Tribologists, Vol. 15/4, pp. 201, 2020

[5] Kostal, D., Okal, M., Fryza, J., Krupka, I., Hartl, M.: Novel in-situ observation of the grease constituents in elastohydrodynamic contacts by fluorescence microscopy, In: Research Square, Vol. 70/4, pp. 126, 2022.

[6] Horiuchi, T., Sakai, Y., Aoyagi, A.: In situ observation of a grease lubricant film on a radial seal by fluorescence induced microscopy, in: Proceedings of the 22nd International Sealing Conference (ISC), Stuttgart, Germany, pp. 459-466, October 1-2, 2024

[7] Kostal, D., Onitsuka, S., Tanaka, H., Sugimura, J., Krupka, I., Hartl, M.: Use of pyrene for quantitative fluorescence observation of Li-grease around EHL contacts, In: Tribology Online, Vol. 15/3, pp. 117-125, 2020.

[8] Delgado, M. A., Secouard, S., Valencia, C., Franco, J. M., On the steady-state flow and yielding behaviour of lubricating greases, In: Fluids, Vol. 4/1, pp. 6, 2019

7 Authors

NOK CORPORATION

4-3-1 Tsujido-shimmachi Fujisawa-shi, Kanagawa, 251-0042 Japan:

Takao Horiuchi, M. Sc., Horiuchi.22.takao@jp.nokgrp.com

Yohei Sakai, M. Sc., Sakai.13.yohei@jp.nokgrp.com

Dr.-ing. Ayako Aoyagi, Aoyagi.07.ayako@jp.nokgrp.com

NOK KLÜBER CO.,LTD.

955-4 Isohara-cho, Isohara, Kitaibaraki-shi, Ibaraki, 319-1541, Japan:

Syunsuke Sato, M. Sc., Sato.15.Syunsuke@jp.nokgrp.com

https://doi.org/10.61319/SWG9RZGF